Research Square

Preprints are preliminary reports that have not undergone peer review.
They should not be considered conclusive, used to inform clinical practice,
or referenced by the media as validated information.

Sensible and Latent Heat Fluxes Over A Processing Cassava Crop with The Surface Renewal and Energy Balance Method

Neilon Silva (neylon.duart@gmail.com)
Universidade Federal do Recôncavo da Bahia: Universidade Federal do Reconcavo da Bahia
https://orcid.org/0000-0002-5558-8898
Aureo Silva de Oliveira
Maurício Antonio Coelho Filho

Research Article

Keywords: coherent structures, temperature ramps, Manihot esculenta

Posted Date: December 30th, 2021

DOI: https://doi.org/10.21203/rs.3.rs-1100769/v1

License: This work is licensed under a Creative Commons Attribution 4.0 International License.
Read Full License

Abstract

There are several methods for determining the sensible heat flux (H) on natural or agricultural surfaces. One such method is the surface renewal (SR) based on ramps of air temperature measured at high frequency by means of an ultra-thin thermocouple. The micrometeorological tower was installed (13°6'39"S, 39°16'46"W, 154 m anm) to assess the suitability of the method in estimating H on industrial cassava cultivation via calibration in relation to the eddy covariance (EC), this consisted of a 3D anemometer. In both systems, measurements were made at a frequency of 10 Hz and comprised the period from 17/04 to 25/07/2019 (100 days). In addition to high-frequency measurements of air temperature and sonic temperature, measurements of net radiation and ground heat flux were also made, and all data grouped at 30-min intervals for determination of latent heat flux (LE) via balance solution power. It was found that (a) the SR method was adequate to estimate the sensible heat flux (H) over industrial matched with a calibration coefficient equal to 0.96; (b) under conditions of unstable atmospheric stability (daytime) the SR method showed better performance for estimating H compared to stable atmospheric conditions (nighttime); (c) the SR method proved to be adequate for estimating the latent heat flux (LE), in the industrial cassava cultivation with a high degree of correlation (r2 > 0.90), with the EC method as a reference; and (d) in the area cultivated with industrial cassava, it was found that the heat flux in the soil (G) corresponded on average to 6% of the radiation balance.

1. Introduction

Understanding the fate of radiative exchanges between the surface and the air is fundamental for modeling the turbulent mass and energy exchange processes that occur in the lower atmosphere (BONAN, 2016). At the surface level, the total radiation balance (Rn) is the energy source for heating the air (H), heating the medium below the surface (G) and for evaporating water (LE). This partition is commonly represented by the simplified energy balance equation [Rn = G + H + LE], where theoretically the difference (Rn – G) is the energy available for turbulent flows (H + LE).

In vegetated areas, LE represents the energy involved in the evapotranspiration (ET) process, a fundamental concept in the context of crop water requirements and irrigation water management. Rn and G can be easily measured with appropriate instruments under field conditions (SNYDER et al., 2008). Obtaining H and LE, on the other hand, is more challenging, as it requires the use of complex and costly instrumentation and requires a method of observation of the turbulence that dominates these two processes in the atmospheric boundary layer (MONTEITH; UNSWORTH, 1990). Detailed description of micrometeorological sensors and procedures for determining turbulent fluxes can be found in Hatfield and Baker (2005), including the energy balance with Bowen ratio,

The surface air renewal (RAS) method is a micrometeorological technique designed to estimate scalar quantities in the atmosphere and has been widely used in the determination of the H component of the energy balance. The method was initially proposed by Paw U and Brunet (1991). Paw U et al. (1995) demonstrated the efficiency of the method in estimating H from fluctuations in air temperature over a

maize crop, a nut orchard and forest. The method is based on the existence of coherent turbulent structures that occur near rough surfaces. Further details on the air renewal method and its development are found in Paw U et al. (2005) and Shaw; Paton; Finnigan, (2013).

The method has been used on a wide spectrum of surfaces. Mengistu and Savage (2010) used RAS to estimate evaporation from a lake in South Africa. The method has been used on vegetation with wide variation in its characteristics such as plant height, age, orientation and planting density as well as openness and canopy architecture. Some vegetated surfaces include forest (PAW U et al., 1995; ZERI; ABREU; NOBRE, 2013), walnut orchard (PAW U et al., 1995), SHAPLAND et al. 2012, POBLETE-ECHEVERRÍA; SEPÚLVEDA-REYES; ORTEGA-FARÍAS, 2014; PARRY et al., 2019), SUVOČAREV et al., 2014), tomatoes (ROSA; DICKEN; TANNY, 2013; XUE et al., 2020), cotton (ROSA; DICKEN; TANNY, 2013), POZNÍKOVÁ et al., 2019), corn (PAW U et al., 1995; XUE et al., 2020), orange orchard (CASTELLVÍ; CONSOLI and PAPA, 2012), and avocado (MORÁN et al., 2020), among others. Once H is determined with the air renewal method, the latent heat flux from the surface in question can be estimated as a residual of the energy balance [LE = Rn – H – G].

The area planted with cassava in Brazil in 2017 was 1.4 million hectares with average productivity ranging from 9.8 to 21.9 t ha-1 (EMBRAPA, 2018) and a national average around 15 t ha-1. Cassava is typically cultivated under rainfall, but when irrigated it can yield twice as much (COELHO FILHO, 2020). To date, there are no reports of the use of the air renewal method to measure the sensitive heat flux H on cassava crops, either under irrigation or under rainfall conditions.

The objectives of this work were (1) to calibrate a surface air renewal system to determine the sensible heat flux over an industrial cassava area; (2) quantify the sensible heat and latent heat fluxes from the crop with the combined methods of surface air renewal and energy balance; and (3) study the partition of the total radiation balance between the components of the energy balance.

2. Materials And Methods

Field experiment location

Fieldwork was conducted at Fazenda Novo Horizonte (13°06'39" S, 39°16'46" W, 154 m asl) in the municipality of Laje, Bahia, Brazil. The total area of the farm is approximately 1000 ha and at the time of this research (2019) it was owned by Bahiamido. The region's climate is transitional between Af (tropical without dry season) and Am (monsoon tropical) according to the Köppen system (ALVARES et al., 2013). The plot where this study was conducted has an area of approximately 10 ha, cultivated with the industrial cassava variety BRS Novo Horizonte. The culture was conducted under a rainfall regime with planting spacing of 90 cm between rows and 80 cm between plants in the row.

Weather tower positioning

The main criterion for choosing a point inside the area for positioning the tower was to ensure sufficient upwind direction. Ease of access to the tower was also considered as a criterion, considering the growth of plants that would make it difficult for personnel to move.

Instruments and data collection

Fast-response and slow-response sensors taken to the field for data colLEECion are listed in Table 1.

Table 1
Fast and slow response instruments installed in the experimental plot

Instrument	Model	Manufacturer	Height or depth (cm)	Parameter measured
Quick answer				
3D sonic anemometer	81000	RM Young	230(a)	Vel. of the wind and sonic temperature (u, v, w, Ts)
ultra thin thermocouple	FW3 (76 µm)	Campbell Scientific	180(b)	Air temperature
slow response				
radiometer balance	NRLite	Kipp & Zonen	270	radiation balance
Pyranometer	SPLite	Kipp & Zonen	270	Solar radiation
flow plate of heat	HFP01	Hukseflux	8	Ground heat flux
ground thermocouple	TCAV	Campbell Scientific	2 and 6	soil temperature
Soil Moisture Meter	GS1	decagon	4	soil moisture
(a), (b) starting height				

Fast response sensors were scanned at a frequency of 10 Hz and data summarized at 30-minute intervals. This was also the integration interval for the data from the slow response sensors, except that these were scanned every 5 s.

Determination of energy balance components

Sensitive heat flux (H)

In the present study, the sensible heat flux density H (W m-2) was determined by two methods: (1) surface air turnover (RAS) and (2) eddy covariance (hereafter referred to as CT). The second was used as a reference for calibrating the first.

Surface Renewal Method (RAS)

Here, this work, the then Surface Renewal, was translated as a method of surface air renewal. Figure 1, adapted from McElrone et al. (2013) illustrates the theoretical formation of air temperature ramps. When a parcel of air comes into contact with the elements of the canopy, it is assumed that a period of quiescence occurs in which there is no variation in the temperature of the parcel (Figures 1a, e). If the plot is cooler than the vegetation then it gains energy and experiences a gradual increase in temperature which is then detected by the ultra-thin thermocouple above the crown (Figures 1b, f). Subsequently, the plot ejects and is replaced (renewed) by another one that is cooler than the vegetation, producing a sharp decline in the temperature trace (Figures 1c, g). From this point, the cycle eventually repeats (Figure 1d, h).

Temperature ramps are characterized by an amplitude (A) and the inverse of the ramp frequency (d + s), as shown in Figure 2, for both conditions of atmospheric stability. Sensitive heat flux density is calculated from these characteristics using an average slope representative of a given time interval, eg 30 minutes, according to Equation 1.

$$H_{RAS} = \alpha \bullet H' = \alpha \bullet \left[\rho C_p \frac{A}{d+s} z \right] \quad (1)$$

where: HSR is the sensible heat flux density after calibration (W m-2); H' is the sensible heat flux density before calibration (W m-2); α is the calibration factor; ρ is the air density (kg m^{-3}); Cp is the specific heat of air at constant pressure (J kg^{-1} $°C^{-1}$); A is the ramp amplitude (°C); 1 / (d + s) is the ramp frequency (s^{-1}) and z is the thermocouple temperature measurement height (m).

Snyder et al. (1996) used statistical moments and the Van Atta (1977) structure function (Equation 2) to calculate the A and (d + s) characteristics of the mean slope, as follows:

$$S^n(r) = \frac{1}{m-j} \sum_{i=1+j}^{m} \left(T_i - T_{i-j} \right)^n \quad \text{(two)}$$

where: m is the number of data points in the 30-minute interval measured at frequency f in Hz; n is the exponent of the function; j is the sampling interval (sample lag) between data points corresponding to a fraction of time (time lag) r given by the ratio (j / f); and Ti is the i-th temperature sample in the 30-minute series. According to Snyder et al. (1996) a condition in Van Atta's (1977) linearized model is that the time fraction r must be much smaller than (d + s).

An estimate of the mean amplitude value A is obtained by solving Equation 3 for real roots.

$$A^3 + pA + q = 0 \quad (3)$$

Where:

$$p = 10S^2(r) - \frac{S^5(r)}{S^3(r)} \quad (4)$$

and

$$q = 10S^3(r) \quad (5)$$

Once the ramp amplitude is known, the inverse of the ramp frequency (d + s) is calculated according to Equation 6.

$$d+s = -\frac{A^3 \bullet r}{S^3(r)} \quad (6)$$

With the values of A and (d + s), 30-minute average values of H' are calculated within the dataloguer program according to Equation 1. A value equal to 1 for the calibration coefficient α is initially assumed, so that the need for calibration can be further evaluated.

Eddie Covariance Method (CT)

In the second method, the sensible heat flux H was obtained using the eddy covariance technique according to Equation 7.

$$H_{CT} = \rho C_p \overline{w'T'} \quad (7)$$

where: HEC is the sensible heat flux density (W m-2) via eddy covariance; ρ is the air density (kg m^{-3}); Cp is the specific heat of air at constant pressure (J kg^{-1} $°C^{-1}$); w' is the instantaneous deviation of the vertical wind speed around the mean (ms^{-1}); and T' is the instantaneous deviation of the sonic anemometer temperature around the mean (°C).

Net radiation and soil heat flux (Rn and G)

As shown in Table 1, the net radiation Rn at the vegetation level was measured with a radiometer balance positioned 270 cm above the ground and mounted on a metallic arm pointing to geographic north.

Two heat flux plates were used to measure the heat flux 8 cm deep and 200 cm away from the tower tripod. One of the plates was installed between plants in the row and the other between rows to better represent the measurements. Soil temperature variation above each plate was monitored with soil

thermocouples inserted at 2 and 6 cm depth while soil moisture within the surface layer was measured with an FDR sensor as described in Table 1.

The heat flux on the soil surface was calculated according to Equation 8.

$$G = G_8 + C_s \left(\frac{T_{s(i)} - T_{s(i-1)}}{\Delta t} \right) z_s \quad (8)$$

where: G is the soil surface heat flux (W m^{-two}); G8 is the ground heat flux measured 8 cm deep; Ts(i) and Ts(i-1) are the mean soil temperatures above the plate at the beginning and end of the time interval Δt, respectively; Δt is the time interval (1800 s); zs is the installation depth of the heat flux plate (m); and Cs is the caloric capacity of the soil (J m^{-3} $°C^{-1}$) calculated with Equation 9 assuming for the experimental area a mineral soil with a particle density of 2.65 Mg m^{-3} and negligible organic matter content.

$$C_v = 2.01*10^6 \rho_s / 2.65 + 4.19*10^6 \theta \quad (9)$$

where: ρs is the density of the soil (1.30 Mg m^{-3}) and θ is the soil moisture (m3 m^{-3}).

Latent heat flux (LE)

The latent heat flux density was obtained as a residual of the energy balance (Equation 10).

$$LE = Rn - G - H \quad (10)$$

where: LE is the latent heat flux density (W m^{-two}) from vegetation; Rn is the total radiation balance (W m^{-two}); G is the soil heat flux density (W m^{-two}); and H is the sensible heat flux density (W m^{-two}). Since measurements of H with air renewal and eddy covariance were obtained independently, the energy balance could be solved for both methods in order to obtain, respectively, LESR and LEEC.

Footprint analysis

A footprint analysis around the micrometeorological tower to delimit the area contributing to turbulent flows was determined based on the model by Kljun et al. (2015) through the FFPOnline tool (v.1.22) found inhttp://footprint.kljun.net/download.php. Zero plane of displacement (d) was calculated as 2/3 of crop height (hc). The Monin-Obukhov length, which is used to characterize atmospheric stability conditions, was calculated according to Equation 13.

$$L = -\frac{\rho C_p \mu_*^3 T}{kgH} \quad (13)$$

where: ρ is the density of air (kg m−3), Cp is the specific heat of air at constant pressure (1004 J kg−1 K−1), u* is the friction velocity (ms−1), T is the air temperature (K), g is the acceleration due to gravity (9.81 ms−2), and H is the sensible heat flux density (W m−2).

3. Results And Discussion

Wind direction and footprint analysis

Figure 3 shows different aspects of the experiment site. Figure 3A is a picture of the tower obtained on 04/30/2019, showing the relative position of the instruments, including the 3D sonic anemometer and the ultra-thin thermocouple (TPUF). Figure 3B shows the compass rose made from 30-minute average data obtained with the sonic anemometer in the period from April 17 to July 25.

The compass rose in Figure 3B shows that the wind blew predominantly (63% of frequency) from the east-south sector with the following distribution: 21% from the south-southeast direction (SSE), 17.4% from the SE direction, 11, 5% from the east-southeast direction (ESE) and 13.2% from the E direction. In each direction, the average wind speeds were 1.13 m s-1 (SSE and SE), 1.23 m s-1 (ESS) and 1.5 m s-1 (E). Figure 3C shows an average footprint for the entire measurement period on an image of the experimental area obtained from Bing, regardless of the change in sonic anemometer height during the period. Overall, the compass rose and the footprint of the turbulent flows are in agreement.

The distance “seen” by the sonic anemometer in the upwind direction totals approximately 50 m on average from the micrometeorological tower. In the prevailing wind direction (SSE) the area of contribution of 90% of turbulent flows is more pronounced.

Calibration of surface air renewal method

Table 2 shows the calibration factor (α), the coefficient of determination (R2) for the regressions through the origin when H of the eddies covariance (HEC) was plotted against the H estimated by air renewal (H'). Data are presented separately for each atmospheric stability condition according to crop growth and change in heights of rapid response sensors and are also presented for the entire measurement period.

Table 2
Calibration of the air renewal method as a function of atmospheric stability conditions and height of rapid response sensors.

atmospheric condition	height of plants (cm)	Height of the TP (cm)	calibration factor	r2 (HEC x H')
Unstable	60 - 150 (a)	180	1.11	0.918
	150 - 200 (b)	200	0.99	0.917
	200 (c)	250	0.87	0.931
	Every period (d)	-	0.98	0.912
Stable	60 - 150	180	0.60	0.783
	150 - 200	200	0.87	0.756
	200	250	0.78	0.669
	every period	-	0.74	0.713
Both	60 - 150	180	1.05	0.886
	150 - 200	200	0.98	0.897
	200	250	0.86	0.897
	every period	-	0.96	0.887

(The) April 17th to May 27th; (b) May 28 to July 1; (c) July 2nd to July 25th; (d) April 17th to July 25th

Under stable atmosphere conditions (H < 0), RAS overestimated the sensible heat flux H' relative to HEC obtained via eddy covariance, resulting in α values consistently lower than 1 in the three intervals (Table 2) and 0.74 for the entire measurement period. For unstable atmosphere conditions (H > 0), α was greater than 1 in the first interval, approximately 1 in the second interval, and less than 1 in the third interval with a seasonal value of 0.98. According to several authors (HU et. al., 2018; McELRONE et. al., 2013; PARRY et. al., 2019), a calibration factor α to correct H obtained via surface air renewal is necessary when there is uneven heating of the soil surface air portion up to the height of measurement of temperature fluctuations. Therefore, based on the seasonal values of α shown in Table 2, it can be said that the method of surface air renewal on the cassava crop performed better for estimating H when unstable atmosphere conditions prevailed. The tendency of RAS to perform better under such conditions was first verified by the method proponents (PAW U et al., 1995) and has been confirmed in several other studies.

Overall, the coefficient of determination (r2) was greater than 0.90 under unstable atmosphere compared to stable atmosphere. Other authors reported values even higher than those in Table 2 (MEKHMANDAROV et. al., 2012; HOLWERDA et. al., 2021).When considering both conditions (unstable + stable) and, therefore, the entire measurement period, the value of α ranged from 0.86 to 1.05 with an average of 0.96,

this very close to 1 and among those found separately for each atmospheric stability condition. The same happened with the values of r2.

Figure 4 graphically illustrates the seasonal calibration of the classical RAS method on industrial cassava crop under both unstable and stable conditions. Figures 4A and 4B show that the agreement between HEC and H' was excellent even before calibration, with a coefficientα of 0.98 as previously shown in Table 2. Under stable atmosphere condition (Figures 4A and 4B), RAS consistently overestimated H (α = 0.74) with higher errors associated with more negative values of H'. But after calibration, HSR became highly correlated with HEC, as expected.

The presence of H values that differ from the other observations (outliers) (Figure 4C and 4D) was more present in the RAS method, in both atmospheric conditions, with emphasis on unstable condition, with a greater number of outliers. At the median level, the values were similar, even before and after calibration, -0.783 W m-2 and 49.347 W m-2 for stable and unstable condition with the RAS method and -0.878 W m-2 and 48.312 W m- 2 for the CT method.

Figure 5 shows the calibration process of the surface air renewal method in relation to the eddies covariance. As mentioned earlier, Figure 5A highlights a calibration coefficient α close to 1 before calibration, which indicates a strong trend of uniform heating and cooling of the air mass from the ground surface to the air temperature measurement heights with the thermocouple ultra-thin, as highlighted byShapland et. al. (2012a, 2012b); Shapland et. al. (2013). Figure 5B shows the calibration result with excellent agreement between HEC and HSR.

The correlation between LEEC and LESR is high (R2 > 0.95) (Figure 5C) as expected as the agreement between HEC and HSR was also high and both LEEC and LESR are calculated from the same set of values of Rn and G. The data suggest that a single calibration coefficient equal to 0.96 can be used for cultivation conditions and climate similar to those presented in this work, with the aim of estimating the sensible heat flux (HSR) in other years of planting provided that the conditions are approximately the same, that is, the same variety is cultivated in the same spacing conducted under rainfed conditions.

Furthermore, the value found for the calibration coefficient α being very close to 1, there is the possibility of using the surface air renewal method with this crop and under the conditions mentioned above without the need for calibration, which in principle would be An ultra-thin thermocouple installed around 50 cm above the crop is sufficient to colLEEC air temperature data and direct application of the air renewal method to determine H.

Energy balance components

The diurnal variations of these components for the months of May and June are shown in Figure 7. For the months under study, the maximum LE values were observed on 05/03/2019 and 06/16/2019, respectively, in the order of 460 .56 and 332.45 W m-2. From the data on global solar radiation, days (13/05 and 17/06) different from those mentioned above were identified, these have high cloudiness,

whose LE values represent the lowest for the period, 180.34 and 65.23 W m-2. For 05/13/2019 and 06/17/2019, the sensible heat fluxes are practically equivalent to the heat flux in the soil, which indicates that there was little energy available to heat the air and the soil, and that 90% de Rn was used for the processes of loss of water to the atmosphere, which is in agreement with Jensen and Allen, (2016) and Gao et. al. (2020).

For both dates 05/03/2019 and 06/16/2019 observed in Figure 7, daily average of G was negative, therefore, all the heat was released to the ground. The opposite situation occurred on the dates of 05/13 and 05/17 when the largest portion of Rs was not converted into LE, which represented about 17.45% and 14.34%, corresponding to an (EF) Evaporative Fraction, EF = LE/(RG) around 56.72% and 51.95%, respectively. For the dates 05/03/2019 and 06/16/2019 the highest available energy resulted in evaporative fraction 79.64% and 69.22% respectively.

Figure 8 shows the relationship between components of the radiation/energy balance in the cultivation of industrial cassava from hourly averages of the data collection period in the experimental area.

Figure 8B shows the relationship between soil heat flux (G) and net radiation (Rn). During the entire period of data collection, which coincided with the vegetative phase of the cassava crop, the degree of ground cover was visually significant, especially because measurements started when the plants had an average height of 60 cm and a predominance of cloudy days. The average value found for the G/Rn ratio was only 6%, which is explained not only by the soil cover by the crop, but also by the proliferation of weeds, considering that the crop was conducted under rainy conditions. In addition to the change in soil water content, the type of cover is a factor responsible for variations in soil heat flux.

Figure 8C shows the relationship between the sensible heat flux obtained via air renewal on the HSR surface and the net radiation Rn. The average H/Rn ratio with this method was around 22%, indicating that most of the available energy must have been used for water evaporation, whose LE/Rn ratio was around 72%, considering that the culture was conducted under rainfall conditions. The period from March to September is the wettest in the region with over 70% of annual precipitation concentrated in these months. Rain data were not collected during the experimental period.

From the point of view of partitioning the energy available for sensible heat fluxes, the values presented here are consistent with those found by Lima et al. (2011) in work carried out with beans in dry conditions. The H/Rn ratio found by the authors ranged between 0.23 and 0.34. In a work involving different types of coverage and associated with the cultivation of cassava, Attarod et al. (2005), using the Bowen Ratio, verified that at the closing of the energy balance the LE/Rn ratio was 0.72 in periods with high water availability and 0.54 in periods of low water availability.

According to Zhou et al. (2012) this high LE/Rn ratio is expected because without water restriction and with a high LAI (current crop phase, 150 DAP) there is an increase in transpiration, thus contributing to higher LE/Rn values and vice versa.

In an area of irrigated cotton Bezzera et. al. (2015), working in a period of high-water availability, found that the LE/Rn ratio was 0.70, with the highest values occurring when the soil was wetter. In this same work, the authors verified that for two consecutive years (2008 and 2009) the G/Rn ratios were 10% and for H/Rn 17% in 2008 and 16% in 2009. Gao et. al. (2020) performed a comparison of evapotranspiration and energy partition related to the main biotic and abiotic controllers in vineyards using different irrigation methods. The authors found that the LE/Rn ratio was 0.75, H/Rn 0.13 and G/Rn equal to 0.12.

Similar values for another crop, that of beans, were reported by Lima et al. (2005), whose LE/Rn ratio was 0.71. Whereas Neves et al. (2008), in the opposite condition of water availability, when quantifying the components of the energy balance in cowpea beans, they found mean values of LE/Rn equal to 0.21, mainly due to the low water availability throughout the crop cycle.

4. Conclusion

1. a) The surface renewal method (SR) method using eddy covariance (EC) as a reference proved to be adequate for estimating the sensible heat flux (H) in the area cultivated with industrial cassava, with a calibration coefficient equal to 0.96.
2. b) Under conditions of unstable atmospheric stability (daytime) the RAS method showed better performance for estimating H compared to stable atmospheric conditions (nighttime);
3. c) The RS method proved to be adequate for estimating the latent heat flux (LE)

Declarations

Funding

This work was supported by Coordenação de Aperfeiçoamento de Pessoal de Nível Superior -Brasil (CAPES) Author A.B. has received research support from Fundação de Amparo e Pesquisa da Bahia (FAPESB).

Competing Interests

Author Neilon Duarte da Silva, Aureo Silva de Oliveira and Mauricio Antonio Coelho Filho, declare they have no financial interests. The authors have no relevant financial or non-financial interests to disclose.

Author Contributions and participate

All authors contributed to the study conception and design. Material preparation, data colLEECion and analysis were performed by Neilon Duarte da Silva, Aureo Silva de Oliveira and Mauricio Antonio Coelho Filho. The first draft of the manuscript was written by Neilon Duarte da Silva, and all authors commented on previous versions of the manuscript. All authors read and approved the final manuscript.

Data Availability

The datasets generated during and/or analysed during the current study are not publicly available due to as they are source of the University Federal oh the Reconcavo of Bahia but are available from the corresponding author on reasonable request..

Code availability

Not applicable

Ethics approval

Not applicable

Consent for publication

The authors agree with the publication of the article and are responsible for the content

Acknowledgments

This work was carried out with the support of the Coordination for the Improvement of Higher Education Personnel (CAPES), Foundation for Research and Support of Bahia (FAPESB) and Embrapa Cassava and Tropical Fruits (EMBRAPA).

References

1. ALVARES, CA; STAPE, JL; SIGN, PC; GONÇALVES, JL de M.; SPAROVEK, G. Koppen's climate classification map for Brazil. Meteorologische Zeitschrift, v. 22, p. 711-728, 2013.
2. ATTAROD P., KOMORI D., HAYASHI K., AOKI M., ISHIDA T., FUKUMURA K., BOONYAWAT S., POLSAN P., TONGDEENOK P., SOMBOON P., PUNKNGUM S. Comparison of the evapotranspiration among a paddy field, cassava plantation and teak plantation in Thailand. Journal of Agricultural Meteorology, vol. 60, p. 789–792. 2005.
3. BEZERRA, BERGSON GUEDES et al. Surface energy exchange and evapotranspiration from cotton crop under full irrigation conditions in the Rio Grande do Norte State, Brazilian Semi-Arid. Bragantia [online]. 2015, v. 74, no. 1 [Accessed 12 September 2021], pp. 120-128. Available from: <https://doi.org/10.1590/1678-4499.0245>. Epub Jan-Mar 2015. ISSN 1678-4499. https://doi.org/10.1590/1678-4499.0245.
4. BONAN, G. Ecological climatology: concepts and applications. 3rd ed. New York: Cambridge University Press. 2016. 740 p.
5. CASTELLVÍ, F.; CONSOLI, S.; PAPA, R. Sensible heat flux estimates using two different methods based on surface renewal analysis. A study case over an orange orchard in Sicily, Agricultural and Forest Meteorology, v 152, p. 58-64, 2012
6. COELHO FILHO, MA Irrigation of the cassava crop. Cruz das Almas: Embrapa. (Technical Release 172). 2020. 12 p.

7. EMBRAPA Cassava in numbers. (https://www.embrapa.br/congresso-de-mandioca-2018/mandioca-em-numeros) Accessed on 12/22/2020.
8. GAO, L., ZHAO, P., KANG, S., LI, S., TONG, L., DING, R., LU, H. Comparison of evapotranspiration and energy partitioning related to main biotic and abiotic controllers in vineyards using different irrigation methods. Front. Ag. Sci. Eng., 2020, 7(4): 490'504 https://doi.org/10.15302/J-FASE-2019310.
9. HATFIELD, JL; BAKER, JM Micrometeorology in agricultural systems. ASA Monograph No. 47. Madison, WI: ASA-CSSA-SSA. 2005. 583p.
10. HOLWERDA, F., GUERRERO-MEDINA, O., MEESTERS, AGCA Evaluating surface renewal models for estimating sensible heat flow above and within a coffee agroforestry system. Agricultural and Forest Meteorology, Volumes 308–309, 2021.
11. HU, Y., BUTTAR, NA, TANNY, J., SNYDER, RL, SAVAGE, MJ, LAKHIAR, IA Surface Renewal Application for Estimating Evapotranspiration: A Review Advances in Meteorology, 11p, 2018.
12. JENSEN, ME; ALLEN, RG Evaporation, Evapotranspiration, and Irrigation Water Requirements. American Society of Civil Engineers, 2nd ed., 2016, 744 p.
13. KLJUN, N., CALANCA, P., ROTACH, MW, AND SCHMID, HP: A simple two-dimensional parameterisation for Flux Footprint Prediction (FFP), Geoscientific. Model Development, v. 8, p. 3695–3713, 2015.
14. LIMA, JRS; ANTONINO, ACD; LIRA, CAPE; SOUZA, ES; SILVA, IF Energy balance and evapotranspiration of cowpea beans under rainfed conditions. Revista Ciência Agronômica, vol. 42, no. 1, p. 65-74, 2011.
15. LIMA, JRS; ANTONIO, ACD; SOARES, WA; BORGES, E.; SILVA IF; LIRA. CAB Energy balance in a soil cultivated with cowpea in Paraíba swamp. Brazilian Journal of Agricultural and Environmental Engineering, v. 09, no. 04, p. 527-534, 2005.
16. MCELRONE, AJ, SHAPLAND, TM, CALDERON, A., FITZMAURICE, L., PAW U, KT, SNYDER, RL Surface Renewal: An Advanced Micrometeorological Method for Measuring and Processing Field-Scale Energy Flux Density Data J Vis Exp. 2013.
17. McELRONE, AJ; SHAPLAND, TM; CALDERON, A.; FITZMAURICE, L.; PAW U, KT; SNYDER, RL Surface renewal: and advanced micrometeorological method for measuring and processing field-scale energy flux density data. Journal of Visualized Experiments. (82), e50666, doi: 10.3791/50666 (2013).
18. MEKHMANDAROV, Y., PIRKNER, M., DICKEN, U., TANNY, J., Examination of the surface renewal technique for sensible heat flux estimates in screenhouses. Acta horticulturae, 923-929, 2012.
19. MENGISTU, MG; SAVAGE, MJ Open water evaporation estimation for a small shallow reservoir in winter using surface renewal. Journal of Hydrology, vol. 380, p. 27-35, 2010.
20. MONTEITH, JL; UNSWORTH, MH Principles of Environmental Physics. 2nd Edition, Butterworth-Heinemann, Elsevier, Oxford, 1990.
21. LIVE IN.; FERREYRA, R.; SELLÉS, G.; SALGADO, E. CACERES-MELLA, A.; POBLETE-ECHEVERRÍA, C. Calibration of the surface renewal method (SR) under different meteorological conditions in an

avocado orchard. Agronomy, v. 10, 730. doi:10.3390/agronomy10050730, 2020.

22. NEVES, LO et al. Energy balance in a cowpea (Vigna unguiculata L.) crop in the state of Pará. Revista Brasileira de Agrometeorologia, v. 16, no. 01, p. 21-30, 2008.
23. PARRY, CK; SHAPLAND, TM; WILLIAMS, LE; CALDERON-ORELLANA, A. SNYDER, RL; PAW U, KT; McELRONE, AJ Comparison of a stand-alone surface renewal method to weighing lysimetry and eddy covariance for determining vineyard evapotranspiration and vine water stress. Irrigation Science, v. 37, p. 737-749, 2019.
24. PARRY, CK, SHAPLAND, TM, WILLIAMS, LE et al. Comparison of a stand-alone surface renewal method to weighing lysimetry and eddy covariance for determining vineyard evapotranspiration and vine water stress. Irrig Sci 37, 737-749, 2019.
25. PAW U, KT, SNYDER, RL, SPANO, D., SU, HB Surface renewal estimates of scalar exchange. In: Hatfield, JL, Baker, JM (Eds), Micrometeorology in Agricultural Systems. Agronomy Monograph no. 47. Amer. Soc. Agron., Madison. pp.455-483., 2005.
26. PAW U, KT; BRUNET, Y. A surface renewal measure of sensible heat flux density. In: Preprints, 20th Conference on Agricultural and Forest Meteorology, 10-13 September, Salt Lake City, Utah, American Meteorological Society, Boston, MA, pp. 52-53., 1991.
27. PAW U., KT; QIU, J.; SU, HB; WATANABE, T.; BRUNET, Y. Surface renewal analysis: a new method to obtain scalar fluxes. Agricultural Forest Meteorology, v. 74, p. 119-137, 1995.
28. POBLETE-ECHEVERRÍA, C.; SEPÚLVEDA-REYES, D.; ORTEGA-FARÍAS, S. Effect of height and time lag on the estimation of sensible heat flux over drip-irrigated vineyard using the surface renewal (SR) method across distinct phenological stages. Agricultural Water Management, v. 141, p. 74-83, 2014.
29. POZNÍKOVÁ, G.; FISCHER, M.; VAN KESTEREN, B.; ORSÁG, M.; HLAVINKA, P.; ŽALUD, A.; TRNKA, M. Quantifying turbulent energy fluxes and evapotranspiration in agricultural field conditions: a comparison of micrometeorological methods. Agricultural Water Management, v. 209, p. 249-263, 2018.
30. ROSA, R.; DICKEN, U.; TANNY, J. Estimating evapotranspiration from processing tomatoes using the surface renewal technique. Biosystems Engineering, v. 114, p. 406-413, 2013.
31. ROSA, R.; TANNY, J. Surface renewal and eddy covariance measurements of sensible and latent heat fluxes of cotton during two growing seasons. Biosystems Engineering, v. 136, p. 149–161, 2015.
32. SHAPLAND, TM; McElrone, AJ; Paw U, KT; SNYDER, RL A turnkey data logger program for field-scale energy flux density measurements using eddy covariance and surface renewal. Italian Journal of Agrometeorology, vol. 18, p. 5-16, 2013.
33. SHAPLAND, TM; SNYDER, RL; SMART, DR; WILLIAMS, LE Estimation of current evapotranspiration in winegrape vineyards located on hillside terrain using surface renewal analysis. Irrigation Science, v. 30, p. 471-484, 2012.
34. SHAPLAND, TM; McELRONE, AJ; SNYDER, RL; PAW U, KT Structure function analysis of two-scale scalar ramps. Part I: Theory and modelling. Boundary-Layer Meteorology, 2012a

35. SHAPLAND, TM; McELRONE, AJ; SNYDER, RL; PAW U, KT Structure function analysis of two-scale scalar ramps. Part II: Ramp characteristics and surface renewal flux estimation. Boundary-Layer Meteorology, 2012b.
36. SHAW, RH; PATON, EG; FINNIGAN, JJ Coeherent eddy structures over plant canopies. In: VENDITTI, JG et al. (eds). Coehrent Flow Structures at Earth's Surface. New York: John Wiley & Sons, 2013. 401p.
37. SNYDER, RL, SPANO, D., PAW U, KT Surface renewal analysis for sensible heat and latent heat flux density. Boundary-Layer Meteorology, vol. 77, p. 249-266,1996.
38. SUVOCAREV, K.; SHAPLAND, TM; SNYDER, RL, MARTÍNEZ-COB, A. Surface renewal performance to independently estimate sensible and latent heat fluxes in heterogeneous crop surfaces. Journal of Hydrology 509 (2014) 83–93, 2014.
39. VAN ATTA, CW Effect of coherent structures on structure and functions of temperature in the atmospheric boundary layer. Archives of Mechanics, vol. 29, p. 161-171, 1977.
40. XUE, J.; BALI, KM; LIGHT, S. HESSELS, T., KISEKKA, I. Evaluation of remote sensing based evapotranspiration models against surface renewal in almonds, tomatoes and maize. Agricultural Water Management, v. 238, 106228. 2020
41. ZERI, M.; ABREU SÁ, LD; NOBRE, CA Estimating buoyancy heat flux using the surface renewal technique over four Amazonian Forest sites in Brazil. Boundary-Layer Meteorology, vol. 149, p. 179-196, 2013.
42. ZHOU, S., WANG, J., LIU, J., YANG, J., XU, Y., LI, J. Evapotranspiration of a drip-irrigated film-mulched cotton field in northern Xinjiang, China. Hydrological Processes, 26, 1169-1178, 2012. http://dx.doi.org/10.1002/hyp.8208.

Figures

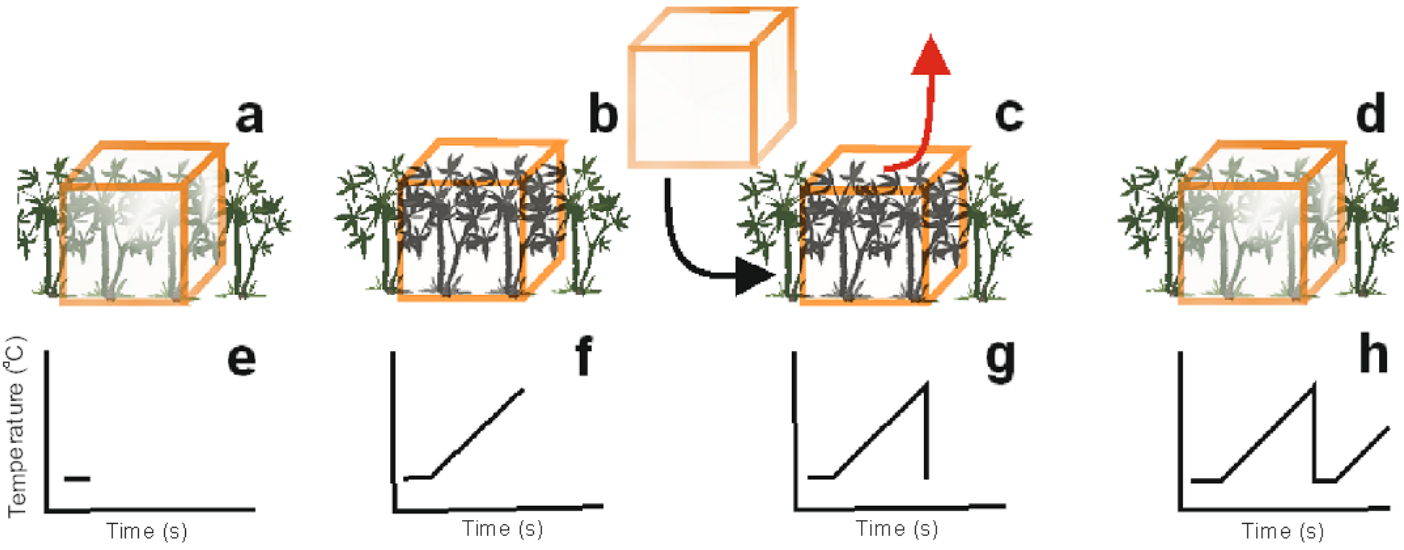

Figure 1

Idealized process of forming air temperature ramps in the surface air renewal method.

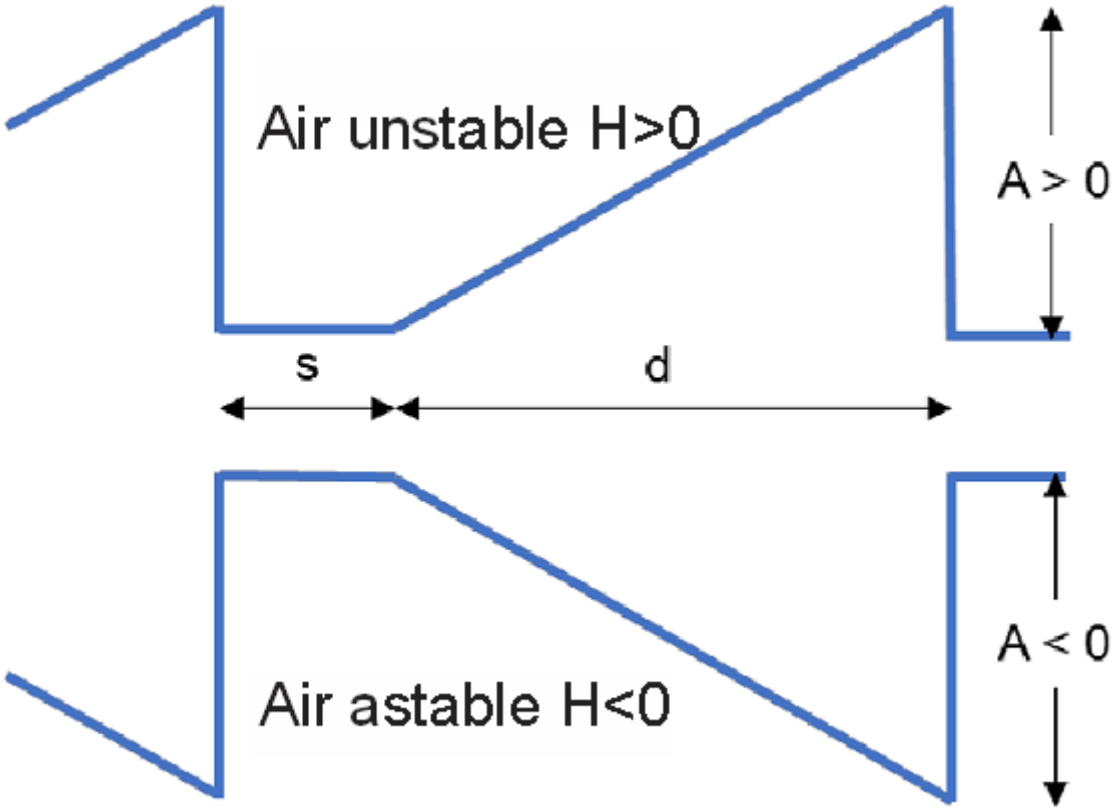

Figure 2

Linearized model of temperature ramps for both unstable and stable conditions, where A is amplitude and (d+s) inverse ramp frequency.

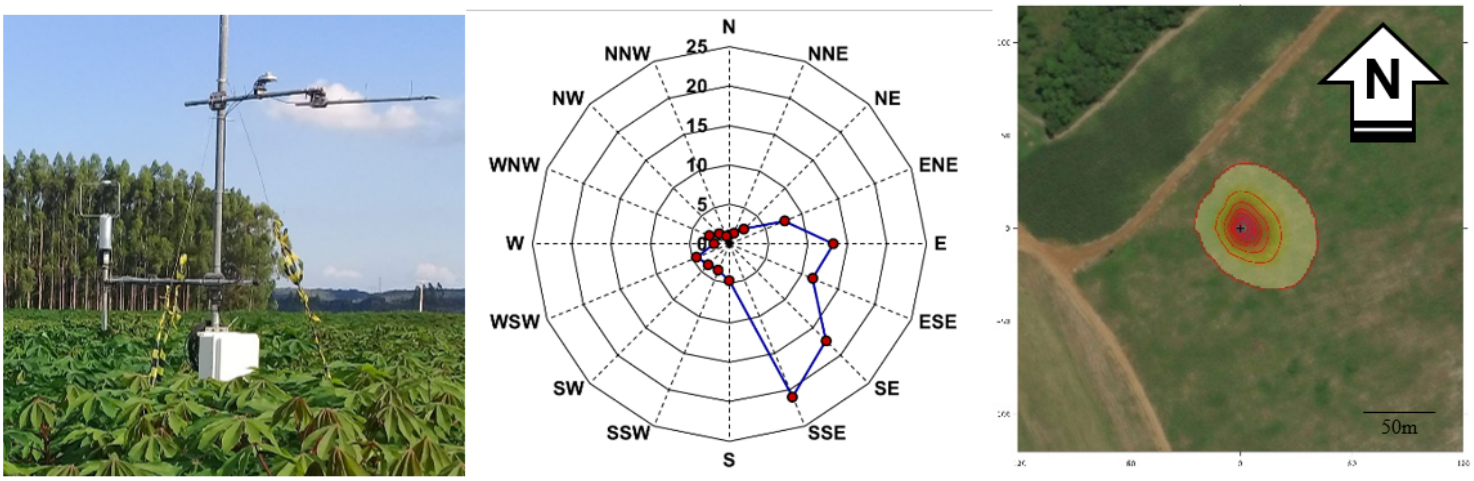

Figure 3

Micrometeorological tower (A); compass rose showing the predominant direction in the experimental area in the period from 17/04 to 25/07/209 (B); footprint analysis (C).

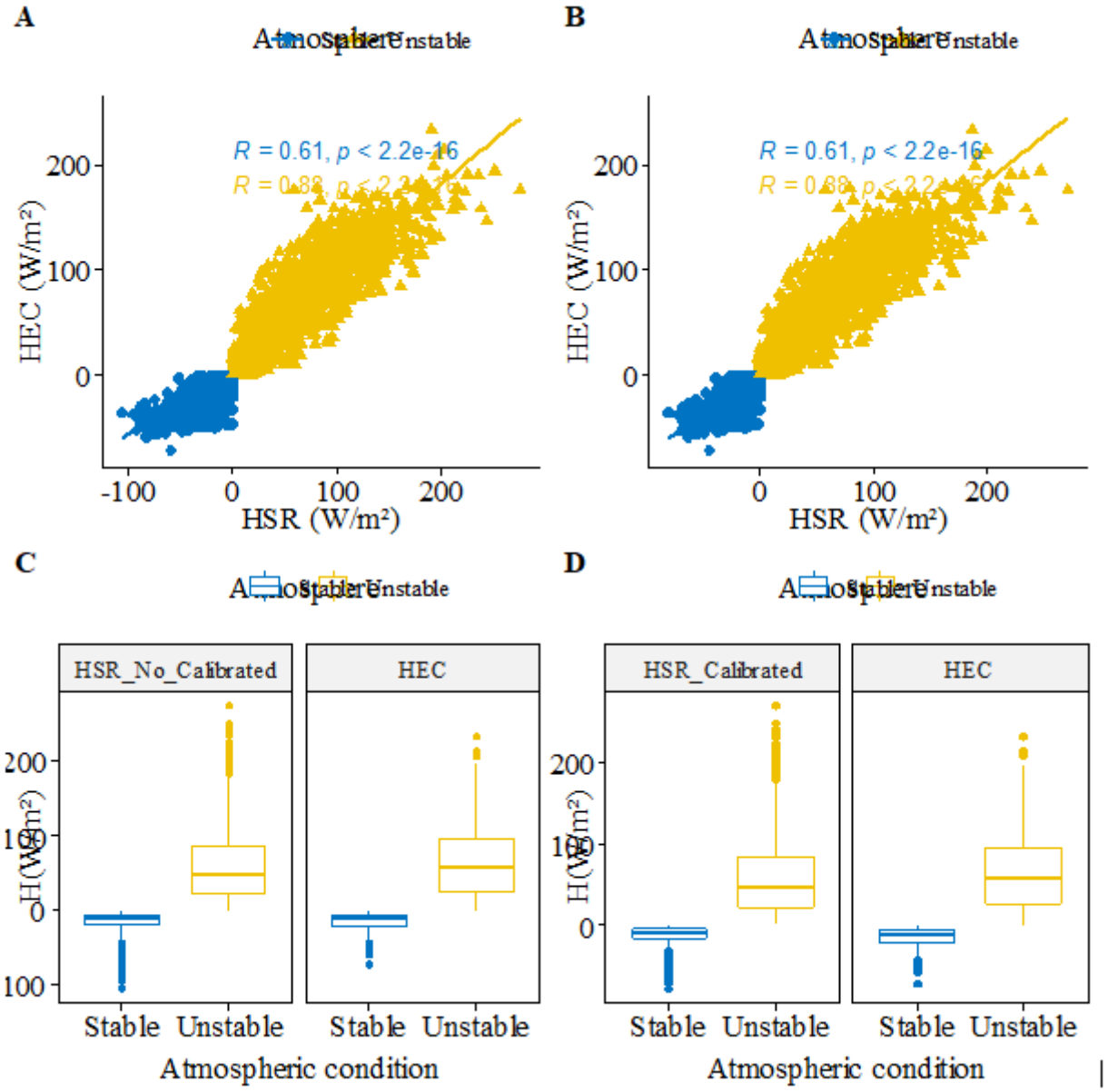

Figure 4

Calibration process of sensible heat flux H' of surface renewal analysis on cassava under stable and unstable atmosphere conditions for all measured data. Before calibration (A and C) and after calibration (B and D).

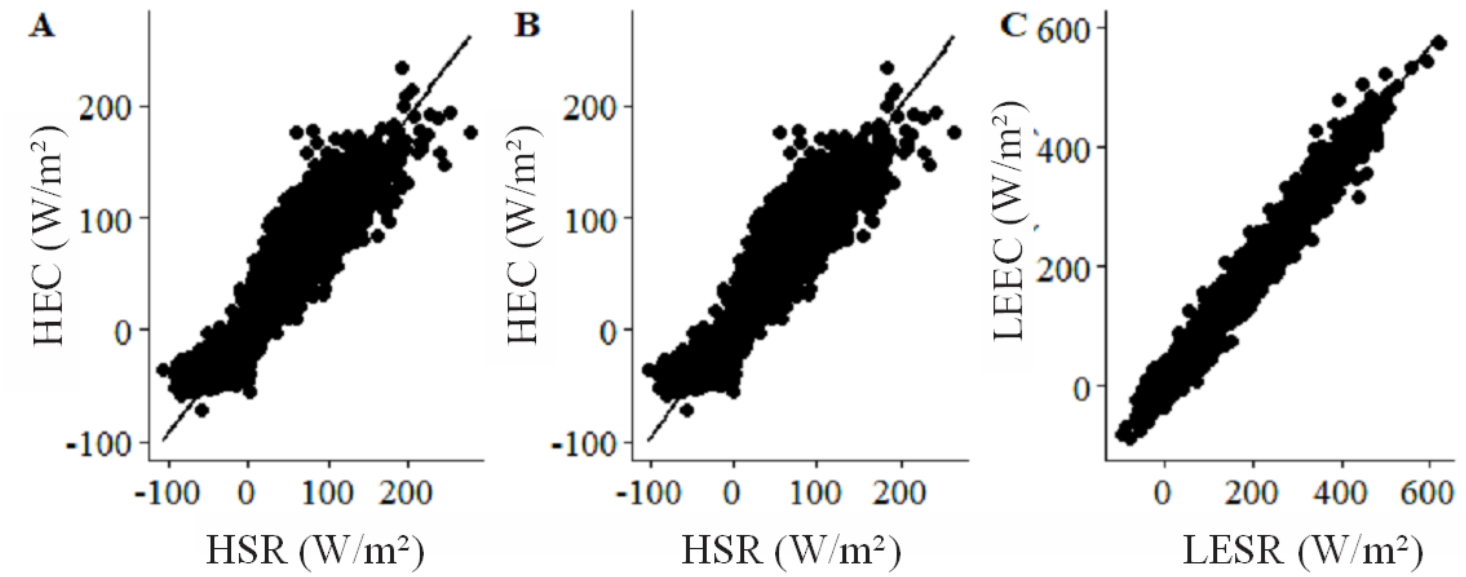

Figure 5

Sensitive heat flux density from turbulent covariance (HEC) versus sensitive heat flux from surface renewal analysis (HSR). Before calibration (A) and after calibration (B). Correlation of latent heat flux between RAS and CT methods (C).

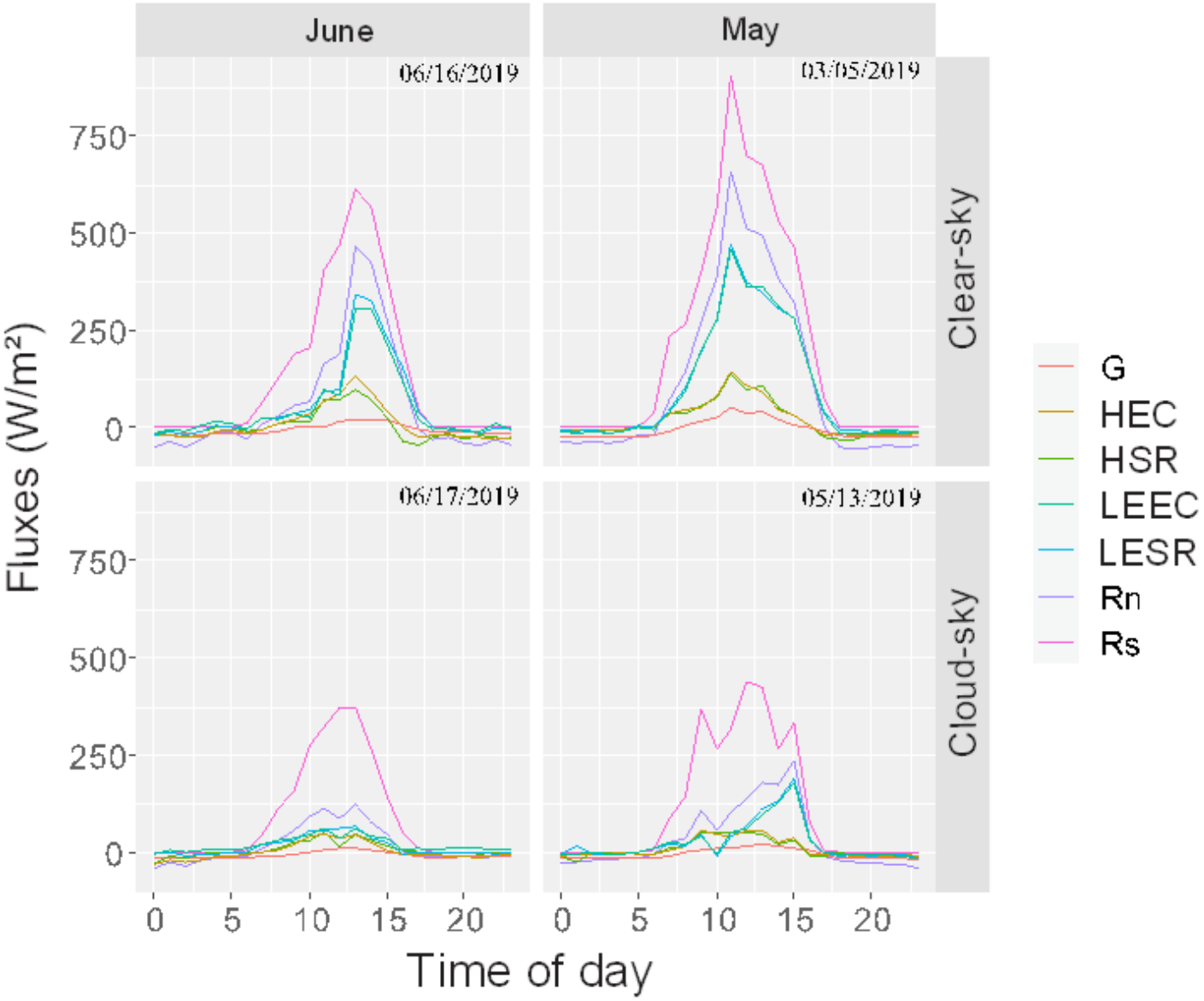

Figure 6

Hourly partition of balance components for different days in May and June under different cloud conditions.

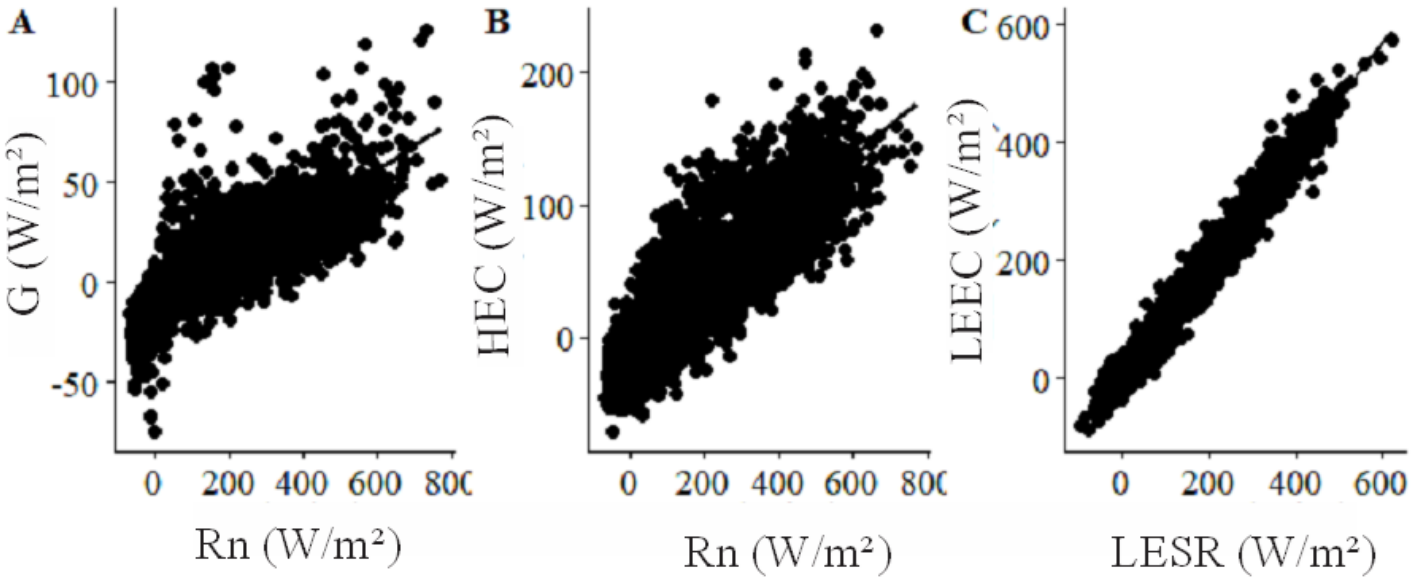

Figure 7

Relationship between net radiation (Rn) and energy balance components (G, H and LE)